Super activation of highly surface segregated dopants in high Ge content SiGe obtained by melt UV laser annealing

Toshiyuki Tabata*[1)], Joris Aubin[1)], Karim Huet[1)], Fulvio Mazzamuto[1)], Yoshihiro Mori[1)], Antonino La Magna[2)], Leonard M. Rubin[3)], Petros Kopalids[3)], Hao-Cheng Tsai[3)], Dwight Roh[3)], and Ronald Reece[3)]
[1)]Laser Systems and Solutions of Europe (LASSE) SASU, SCREEN Semiconductor Solutions Co. Ltd, 14-38 rue Alexandre, Bldg D, F-92230 GENNEVILLIERS, France
[2)]CNR IMM, Z.I VIII Strada 5, I 95121 Catania, Italy
[3)]Axcelis Technologies, Inc. 108 Cherry Hill Drive, Beverly, MA 01915 USA.
*toshiyuki.tabata@screen-lasse.com / +33 6 42 27 21 77

***Abstract*—Activation of surface segregated dopants above the solid solubility limit in a high Ge content SiGe substrate has been demonstrated by nanosecond melt UV laser anneal. This exceeds the activation possible with conventional solid-phase annealing technics. The segregation effects, strongly amplified by the phase changing of the partial melting of the sample during the annealing, play a key role explaining dopant profile redistribution in Si-Ge alloys and activation.**

***Keywords*—laser annealing, contact, segregation, activation**

I. Introduction

In advanced nodes, the contact area of transistors becomes so small that the metal-semiconductor contact resistivity dominates the parasitic factor [1]. To overcome it, contact resistivity can be improved by high-dose ion implantation and/or in-situ doping during epitaxial growth [2-3]. Moreover, melt laser annealing (MLA) is known to enable a dopant activation over the solid solubility limit thanks to an ultrafast (sub-µs) melting and recrystallization process [4-5]. In this context, MLA is of great interest for lowering contact resistance in future nodes. When the segregation coefficient (k) of dopants in a semiconductor material is much lower than 1.0, another benefit can be expected from MLA: the dopant profile can be optimized by taking advantage of the surface segregation phenomena. This application is particularly interesting for SiGe p-type contacts. This is because the active boron concentration in the SiGe layer, especially for a high Ge content, will be limited by its lower solid solubility in Ge [6] than in Si [7]. Other than B, a group-III element like gallium is a good candidate with a low segregation coefficient ($k << 1$) both in Si [8] and in Ge [9-10].

However, when introducing dopant atoms into a crystal lattice over their solubility limit, there is a risk of forming defects which may result in a worse activation of dopants and/or of losing thermal stability of the activated dopants. In the case of MLA of Ga-implanted Si, the solid solubility limit of Ga in Si (4.5×10^{19} cm^{-3}) can be extended by an order of magnitude higher (4.5×10^{20} cm^{-3}) [4]. Incorporation of the excess dopant to interstitial sites is suspected. The maximum substitutional solubility that can be achieved by MLA appears to be limited by three mechanisms [11]: (i) a lattice strain related to the covalent bonding radius of the dopant, (ii) an interfacial instability that is caused by constitutional super-cooling in front of the liquid-solid interface and related to an unstable perturbation of the interface, and (iii) a thermodynamic limit concerning a diffusion-less solidification process. When the concentration of the dopant involved in a non-equilibrium solidification from the liquid phase is very high with high velocity, a liquid solubility limit can be understood only in a very complex way as explained above. Furthermore, the distribution coefficient of an element changes depending on the solidification velocity [12]. If there are different elements diffusing in the molten layer, it adds additional complexity to the solidification dynamics.

In this work, we report the surface segregation and activation of Ga atoms doped in a high Ge content SiGe epitaxially grown layer, after MLA using our UV excimer laser annealing equipment (LT-3100). Results are discussed with the support of our in-situ methodology (the time-resolved reflectivity (TRR) monitoring system) and in-house simulation software (Lasse Innovation Application Booster (LIAB)) specifically developed for MLA process.

II. Experimental

A 300mm n-type Si(100) prime wafer was used as a substrate. A 300mm Epsilon 3200 Reduced Pressure Chemical Vapor Deposition tool (ASM America) was used to grow a 66nm thick SiGe 50% layer on the substrate, with a growth pressure kept at 20 Torr. Purified H_2 was used as carrier gas flow (several tens of standard liters per minute). The SiGe layer was grown at 550°C, using a SiH_4 + GeH_4 chemistry. The deposited film thicknesses were controlled using a fully automated Jordan Valley X-Ray Reflectivity tool. The deposited SiGe is partially relaxed and the macroscopic degree of relaxation is estimated to be 30-40% [13]. Gallium was then ion-implanted as a dopant (26 keV, at room temperature (RT)), to a nominal dose of ~1×10^{16} at/cm^2. The impurity projected range, R_p, was located at a depth close to 20nm. 308 nm UV excimer laser annealing was applied with different laser energy densities (ED) on the samples at RT. The pulse duration was controlled to be 160 ns. The dopant profile before and after MLA was measured by SIMS. The dopant activation was studied by four point probe and electrochemical capacitance-voltage profiling (ECVP) [14-15] techniques.

III. Results and discussion

A. *Process monitoring during LTA*

When a SiGe is irradiated by a pulsed laser, the surface starts melting after a certain ED (J/cm^2) and the depth of the

molten layer increases progressively with increasing ED. Figure 1 shows a set of TRR signals obtained during the MLA process on our SiGe samples with different EDs. While the sample surface is liquid, it shows a higher reflectivity than when it is solid. It is clearly seen that the melting time (the full width at half maximum of the TRR signal peak) becomes longer with increasing ED, meaning that the melting depth is increasing. From a plot of the melting time vs. ED, a threshold ED of melting can be determined by extrapolation. An approximate melt front velocity can be estimated by dividing the full distance of melt evolution and recrystallization (i.e. 120nm for the 60nm thick SiGe layer) by the melting time. In our case, it was less than 1 m/s, where Ga has a distribution coefficient of less than 0.1 [12]. The first abrupt peak shown at around 190 ns can be attributed to an explosive melting of the SiGe surface which has been amorphized during ion implantation [16]. The difference between the initial and final signal intensities indicates a modification of the surface. An increase of Ge concentration near the surface during the MLA may be the cause of the final signal intensity being larger than the initial. This is consistent with the fact that the distribution coefficient of Ge in Si at the melting point of Si is about 0.33 [7]. On the other hand, when the melting depth goes through the Si substrate, the final signal intensity may be decreased because of Ge diffusion into the Si substrate. Also, increased surface roughness may decrease the final signal intensity.

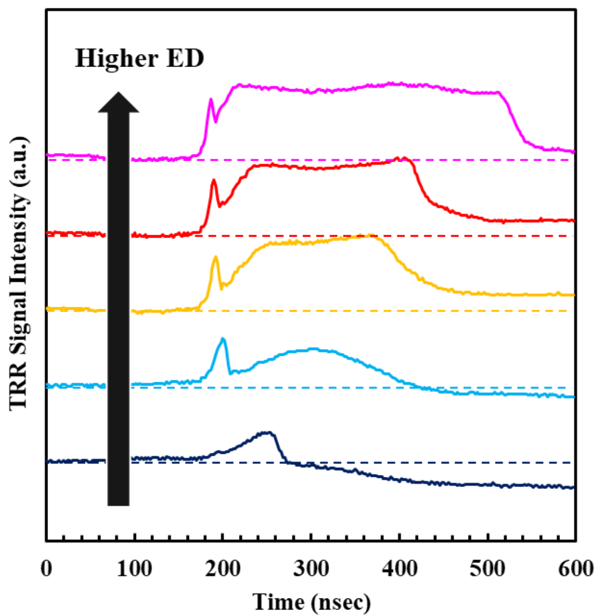

Fig. 1. TRR signals obtained during the MLA process of the Ga-doped SiGe layer.

B. Surface segregation of Ga in SiGe

Figure 2 shows the SIMS profiles of Ga for the non-annealed and annealed samples. The melting depth was extracted for the annealed samples by observing the pile-up of the oxygen profile [17]. Since there is very little oxygen in an epitaxial film, the source of oxygen is believed to be the native oxide on the SiGe surface, from which some oxygen atoms were knocked-on by the Ga atoms during implantation. The evolution of the melting depth is reported for each ED. The implanted Ga atoms are strongly segregated towards the surface even with a shallow melting of the SiGe layer. As shown in Figure 3, this segregation seems to correspond well to the Ge distribution after MLA. Considering that the equilibrium distribution coefficient of Ga in Ge (0.071 - 0.078 [7, 10]) is larger than that in Si (0.008 [8]), the higher liquid solubility limit of Ga in Ge than in Si would allow such a high concentration. A quantitative comparison of Ga concentration over the profiles would be incorrect because of the variation of Ge concentration in the film after MLA, which induces a matrix effect. Apart from surface segregation, the implanted Ga atoms seem to diffuse also in the solid phase, which is not likely given the very short timescale of the process. As evidenced by the TRR signals, an explosive crystallization phenomenon occurs at the beginning of the melting process, crystallizing the whole amorphized layer at very high velocity [16]. As shown in Figure 4, at the early stage of pulsed laser heating, the explosive melt front may redistribute the dopants within the whole SiGe layer, resulting in a nanocrystalline layer (Fig. 4(b)). If the heating source is sufficiently intense, this nanocrystalline layer melts again with a more traditional melting process and the dopants are then redistributed only within the molten region (Fig. 4(c)).

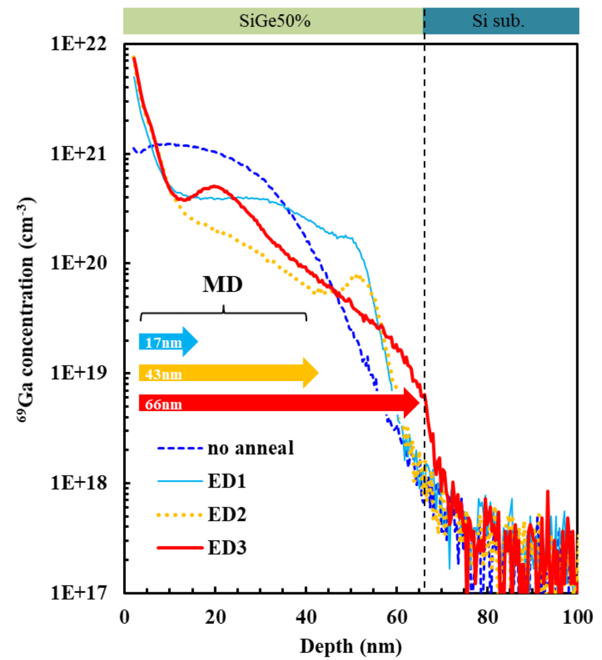

Fig. 2. ^{69}Ga SIMS profiles of the non-annealed and annealed samples, where the melting depth (MD) was determined by the pile-up of the O profile (not shown).

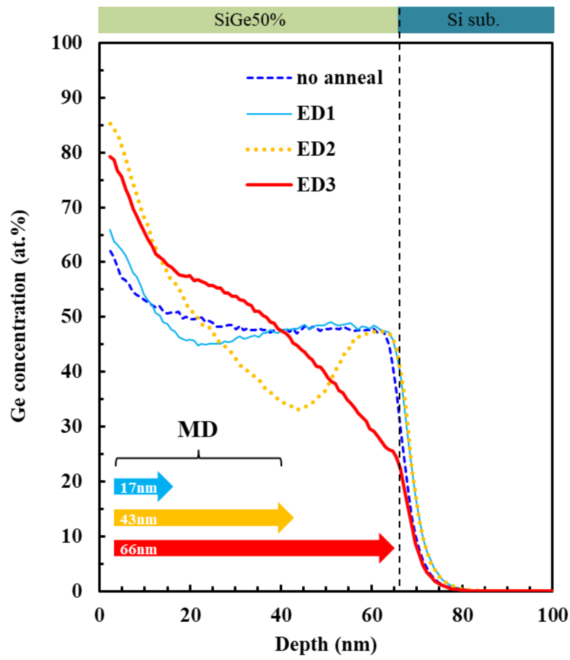

Fig. 3. Ge SIMS profiles of non-annealed and annealed samples, where the melting depth (MD) was determined by the pile-up of the O profile. The Ge concentration is converted to at. % in $Si_{1-x}Ge_x$.

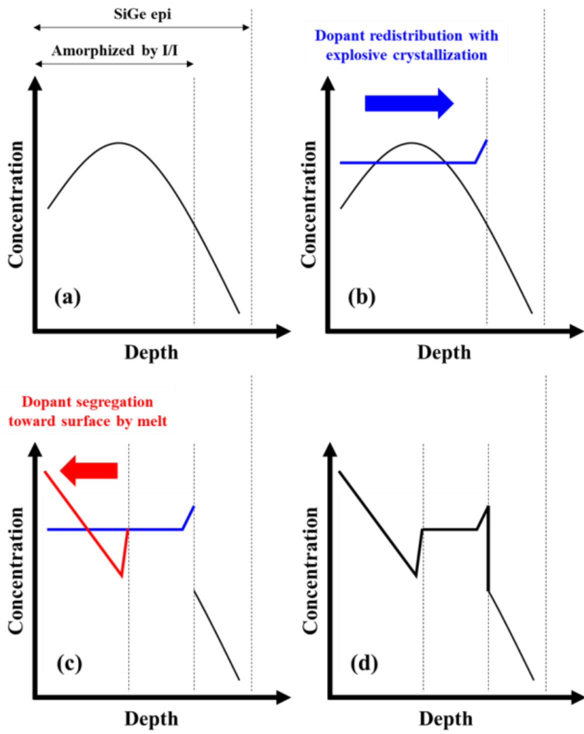

Fig. 4. Schematic figure of the dopant redistribution by explosive crystallization and melting during the partial MLA process: (a) as-implanted, (b) explosive crystallization, (c) segregation by melting, (d) finally obtained dopant profile after the partial MLA process.

C. *Simulation of surface segregated Ga in SiGe*

Our in-house simulation tool, LIAB, may help to understand what happens during the Ga segregation demonstrated above. In LIAB, the heating of the UV laser annealing process is evaluated by means of a self-consistent solution of the time harmonic solution of the Maxwell equations and the self-consistency derives from the dependence of the optical constant on the temperature, the phases (amorphous, crystal, and liquid) and the alloy fraction [18-19]. The LIAB package integrates the open-source numerical solver FEniCS [20-21] to solve partial differential equations and includes a multiple-dopant model simulating diffusion, solubility, and segregation of atoms in the different phases as well as a SiGe alloy model. It should be noted that explosive crystallization cannot be simulated yet.

Based on the material properties reported previously (i.e. the solid solubility limit of Ga in Si [7] and Ge [7], the equilibrium distribution coefficient of Ga in Si [8] and Ge [7, 10]), we have simulated the Ga diffusion in the SiGe 50% layer and compared it with the SIMS profiles. Each material property was converted to a value of SiGe 50%, assuming that it follows Vegard's law. The Ge redistribution in SiGe during MLA was calibrated by some experimental results reported elsewhere [22]. As a fitting parameter, we changed the liquid solubility limit of Ga in molten SiGe so that it becomes 1X, 2X, and 10X the value in solid SiGe. Figure 5 shows that the liquid solubility limit has a large contribution on the obtained profiles. When the liquid solubility limit is set to 10X larger than the solid value, the simulated segregation profile shows very good agreement with experiment. On the other hand, since explosive crystallization is not considered, the diffusion of dopants in the non-molten region is not well reproduced. As mentioned above, such enhancement of the solubility limit in liquid phase has been demonstrated by experiment [4]. Thus, due to the extreme solubility limit in the liquid phase realized by MLA, we expect that most of the Ga segregated near the surface is substitutional and activated. Indeed, a sub-$1x10^{-9}$ $ohm.cm^2$ has been achieved by a combination of Ga ion-implantation and MLA [5].

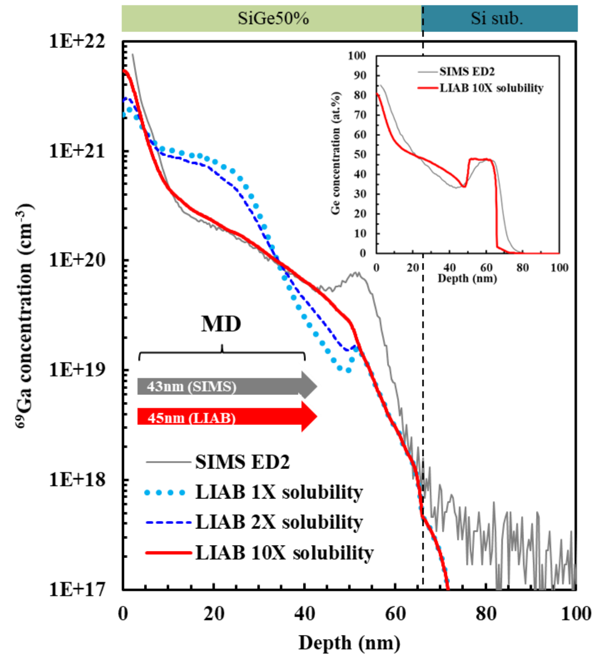

Fig. 5. ^{69}Ga SIMS and LIAB profiles after MLA, where the liquid solubility was varied as a fitting parameter. The melting depth (MD) was determined by the pile-up of the O profile.

D. *Activation of surface segregated Ga in SiGe*

To investigate the activation of Ga doped in the SiGe 50% layer, we used ECVP [14-15]. The measurement was done on a Biorad PN 4300 equipped with an O ring of 1 mm^2 and with the electrolyte HCl 0.5 M/l + NH_4FHF 0.1 M/l. The capacitance measurements were performed every 2-3 nm etching in depth. The reverse voltage was set at about 0.1V,

which gave a space charge zone depth equal to 1-2nm. With such a low voltage, the contribution of deep levels (mostly deep acceptors) on the measured capacitance can be minimized as much as possible [23].

Figure 6 (a) and (b) show the active dopant profiles for the samples annealed at ED1 and ED3 as compared with the SIMS profiles and the solid solubility limit of Ga in $Si_{1-x}Ge_x$. In Fig. 6 (b), we can clearly see that the Ga atoms are fully activated because its concentration is below the solid solubility limit in the bottom-half of the SiGe layer. However, in the top-half of the SiGe layer, the activation is restricted by the solid solubility limit and there are many excess dopants which are not active and probably at interstitial sites. In Fig. 6 (a), we can see that the Ga atoms are not totally activated in the non-molten SiGe layer but the active dopant concentration increases monotonically towards the interface between the molten and non-molten layers until it reaches at the solid solubility limit. This can be explained by the thermal gradient in the non-molten SiGe layer induced during the MLA process. Surprisingly, the concentration of active dopants becomes about 6 times higher than the solid solubility limit near the surface, indicating that the enhanced solubility limit in liquid allows for incorporating the dopants onto substitutional sites and making them active. In this case, the velocity of the liquid/solid interface during recrystallization would play a key role. From LIAB simulation, this velocity is two times smaller in the MLA process at ED1 than at ED3. If so, a small enough velocity of the liquid/solid interface will help stabilize the active substitutional sites over the solid solubility limit and will further improve the contact resistivity.

IV. Conclusion

Activation of Ga in SiGe over the solid solubility limit has been demonstrated by using MLA. The equilibrium segregation coefficient (k) of dopants in Si and Ge can be used to predict segregation in a high Ge content SiGe epitaxially grown layer. Our new in-house simulation software, LIAB, has closely reproduced the experimental profiles of the segregated dopants as well as the Ge diffusion in the molten SiGe layer. The solubility limit of dopants becomes 10 times larger in the liquid than in the solid phase. It seems that the activation after the segregation much depends on the velocity of the liquid/solid interface during recrystallization in the MLA process. We believe that the MLA process has not been optimized yet and there is still an opportunity for improvement.

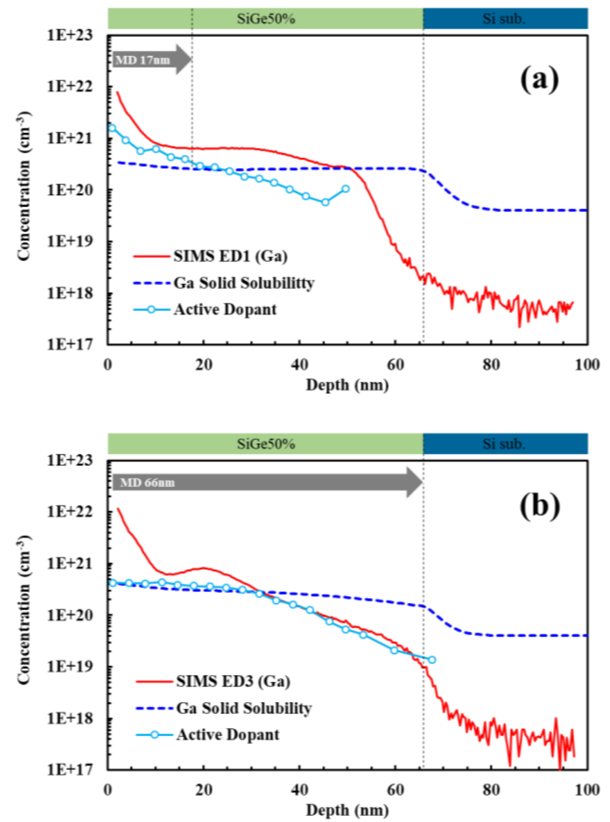

Fig. 6. Active dopant profiles obtained by ECVP as compared with the SIMS profiles and the estimated solid solubility limit of Ga atoms in the SiGe layer after MLA. The MLA process was performed (a) at ED1 and (b) at ED3. The melting depth (MD) was determined by the pile-up of the O profile. The total concentration of ^{69}Ga and ^{71}Ga is shown for the SIMS profiles.

References

[1] P. Raghavan et al., IEEE CICC 2015, p.1..
[2] M. Sinha et al., IEEE Trans. Electron. Devices, 57, p. 1279 (2010).
[3] S. N. R. Kazmi et al., ECS J Solid State SC, 1, p. 222 (2012).
[4] J. M. Poate and James W. Mayer, “Laser Annealing of Semiconductors”, Academic Press, p. 130 (1982).
[5] J-L. Everaert et al., VLSI 2017, p. T214.
[6] S. Uppal et al., J. Appl. Phys, 90, p. 4293 (2001).
[7] F. A. Trumbore, The Bell System Technical Journal, 39, p. 205 (1960).
[8] M. Liaw et al., "Sequential Purification and Crystal Growth for the Production of Low Cost Silicon Substrates", U.S. Department of Energy, Quarterly Technical Progress Report No.3, p. 6 (1980).
[9] F. A. Trumbore et al., J. Phys. Chem. Solides, 11, p.239 (1959)
[10] J. P. Garandet, J. Crystal Growth, 310, p. 3268 (2008).
[11] C. White et al., “Laser and Electron Beam Solid Interactions and Materials Processing”, North-Holland Publ., New York, p. 59 (1981).
[12] R. F. Wood, Appl. Phys. Lett., 37, p. 302 (1980).
[13] J. M. Hartmann et al., J. Appl. Phys., 110, 083529 (2011).
[14] P. Blood, Semicond. Sci. Technol., 1, p. 7 (1986).
[15] E. Peiner et al., J. Electrochem. Soc., 142, p. 576 (1995).
[16] S. F. Lombardo et al., J. Appl. Phys., 123, 105195 (2018).
[17] R. Monflier et al., in preparation.
[18] A. La Magna et al., Proc. of the FEniCS conference 2017, #32.
[19] A. La Magna et al., Proc. of the E-MRS Spring Meeting 2018.
[20] M. Alnæs, et al., “The FEniCS Project Version 1.5,” Archive of Numerical Software, 3 (100), 2015.
[21] A. Logg et al., “Automated solution of differential equations by the finite element method: The FEniCS book,” Vol. 84. Springer Science & Business Media, 2012.
[22] L. Dagault et al., to be published.
[23] B. Sermage et al., J. Appl. Phys. 119, 155703 (2016).